Vortex Dynamics and Melting in Niobium

J. W. Lynn,[1,2] N. Rosov,[1] T. E. Grigereit,[1,2] H. Zhang,[1,2] and T. W. Clinton[2]

[1]*Reactor Radiation Division, National Institute of Standards and Technology, Gaithersburg, Maryland 20899*

[2]*Center for Superconductivity Research, Department of Physics, University of Maryland, College Park, Maryland 20742*

(Received 27 October 1993)

Small angle neutron scattering has been used to investigate the vortex scattering in single crystal niobium. In the mixed state ($H_{c1} < H < H_{c2}$) a sixfold hexagonal pattern of peaks is observed at all temperatures. Below the irreversibility line these peaks are resolution limited, while above it the width in the transverse direction increases with temperature due to the vortex dynamics. Close to H_{c2} the radial widths of the peaks also broaden. However, the basic hexagonal pattern of peaks is maintained throughout, indicating that a correlated flux fluid exists in the reversible regime.

PACS numbers: 74.60.Ge, 61.12.Ex, 74.25.Dw, 74.70.Ad

One of the most interesting and fundamental questions concerning the vortex structures in superconductors is whether or not they undergo a melting transition. Early work in the cuprate systems identified an irreversibility line [1], suggesting that the basic vortex behavior was quite different than for conventional superconductors [2]. In the low field regime below the irreversibility line (T_{irr}) the vortices are thought to exist in a lattice or glass, while in the high field regime above T_{irr} they melt into some kind of a fluid phase. However, it has proved difficult to probe the structure of these phases directly because techniques such as Bitter decoration are restricted to low fields [2], while neutron scattering experiments [3,4] have suffered from the low signal to noise presently available for high T_c samples. This melting behavior was thought to originate from the unique physical properties of the cuprates [5–10], namely, the large κ, intrinsic anisotropy, and high thermal energies available near T_c, but a reexamination of conventional superconductors has revealed that they also undergo a melting phenomenon [11–13]. We have therefore been carrying out an extensive series of small angle neutron scattering measurements on a high quality single crystal of niobium, where the signal to noise is several orders of magnitude better than currently available from the best high T_c crystals. The high quality of the present data has allowed us to observe broadening of the vortex peaks, first in the vicinity of the irreversibility line, and then again close to H_{c2}. The basic sixfold symmetry of the scattering, however, is preserved throughout the vortex regime, indicating that a correlated flux fluid exists rather than a conventional isotropic fluid.

The experiments were carried out on the NG-3 and NG-7 30 m small angle neutron scattering (SANS) spectrometers in the Cold Neutron Research Facility at NIST. The sample was a high purity single crystal of Nb in the form of a cylinder 1.25 cm in diameter and 9 cm long, with the [110] crystallographic axis along the cylinder axis. Two experimental setups were employed, one with an electromagnet ($H \leq 0.5$ T) and a cryostat ($T \geq 4.5$ K) placed between the pole pieces, and a second superconducting magnet system ($H \leq 9$ T, $T \geq 1.5$ K) specially designed for SANS studies. In both cases the field was applied approximately parallel to the incoming and exiting neutrons, and perpendicular to the cylinder axis. The beam diameter was typically 1 cm, illuminating the center portion of the crystal. The field was applied in a variety of directions within the [*hhl*] scattering plane, with similar results; here we will concentrate on the results obtained with H parallel to the [110] type direction [14]. Both isothermal and isomagnetic scans were performed.

Figure 1 shows the basic scattering pattern observed on the two-dimensional position sensitive SANS detector,

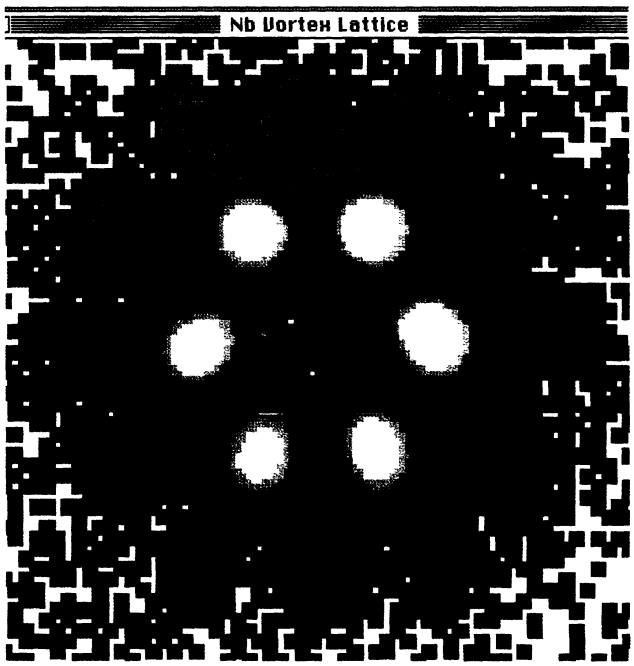

FIG. 1. Image on the two-dimensional SANS detector, taken with relatively coarse resolution. The log of the scattered neutron intensity has been mapped into a color spectrum. The sixfold pattern of first-order peaks has the strongest intensity, with higher order peaks having weaker intensities.

0031-9007/94/72(21)/3413(4)$06.00

plotted using a logarithmic pseudocolor mapping. In the center of the image is a beam mask which catches the undeviated neutron beam. A sixfold pattern of Bragg peaks from the vortex lattice occurs at a momentum transfer Q_0, along with (weaker intensity) higher order magnetic peaks that appear at larger Q. These are raw observed counts, obtained in 2 min counting time, and demonstrate the high quality of the data that can be obtained on niobium. These data can be compared with results for $YBa_2Cu_3O_7$, which require several hours of counting at each (H,T), and then the vortex pattern is evident only after a subtraction of a zero-field-cooled background measurement to determine the scattering from defects such as grain and twin boundaries, flux inclusions, etc. [3,4]. Thus if the vortex lattice in Nb indeed melts, this system offers us the best opportunity to observe it directly via SANS.

There are several types of information that can be obtained from data such as shown in Fig. 1. The radial position of the peaks is directly related to the vortex flux quantum and the density of flux lines in the sample. The widths of the peaks can be obtained in both the radial and transverse (angular) directions, and the intensity can be monitored, all as a function of (H,T). For example, the intensity of the scattering at the radial peak position Q_0 is plotted in Fig. 2(a) as a function of the angle ϕ around the detector. Six distinct peaks, separated by 60°, are observed at this temperature (6.5 K) and applied field (0.2 T). The integrated intensity of the vortex scattering as a function of temperature is shown in Fig. 2(b) for the same field. The data demonstrate that the scattering intensity changes smoothly and continuously with temperature. In particular, we do not observe any discontinuous behavior such as might be expected in a first-order melting transition [5,9]. We also note that the intensity of the vortex scattering intensity does not fall steeply near T_c (or T_{melt}). The inset shows the same intensity plotted on a linear scale, where we see that the scattering approaches tangentially the temperature axis as $T \rightarrow T_c$. Thus in raw SANS data there is no obvious way to identify any type of transition. This is particularly important to keep in mind for the high T_c materials, where the signal would be lost at much lower relative temperatures than in the present case. Finally we note that in addition to the Q widths discussed above, the entire intensity pattern can be measured as the sample and magnet are rotated (rocking curve). In this geometry such data are related to how parallel and straight the vortices are in the sample. Typically we obtain rocking curves of between 12 and 18 ft FWHM, indicating that the lattice is very well formed and the vortices are straight and parallel over the entire (H,T) range where magnetic scattering can be observed.

The temperature dependence of the observed Q widths of the magnetic vortex peaks is shown in Fig. 3, obtained by cooling in an applied field of 0.2 T. At low temperatures these widths are instrumentally limited, and this is

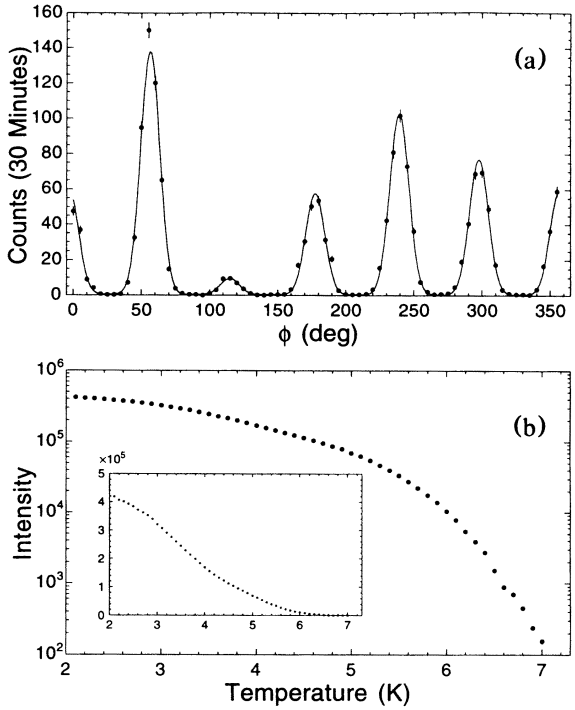

FIG. 2. (a) Intensity of the vortex scattering at the peak position as a function of the angle around the detector, measured with the highest available resolution at 6.5 K and 0.2 T. Six peaks separated by 60° are readily evident, while the (transverse) widths of the fitted curves reveal that the peaks have an intrinsic width at this temperature. (b) Temperature dependence of the vortex scattering, showing that the intensity varies continuously with temperature. The inset is the same data plotted on a linear scale.

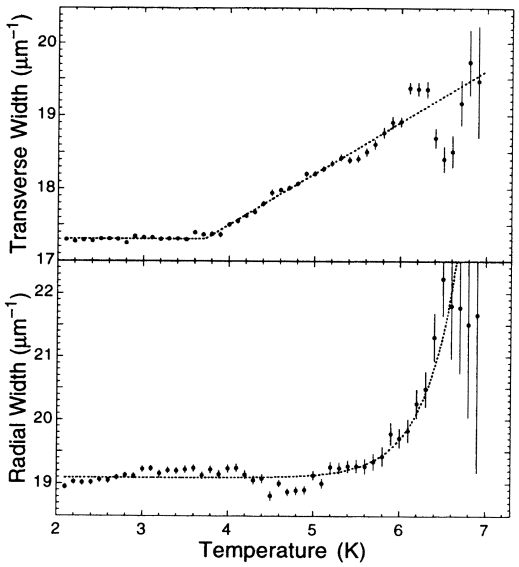

FIG. 3. Measured radial and transverse (angular) widths as a function of temperature for an applied field of 0.2 T. The widths at low T are resolution limited. The solid curves are a guide to the eye.

the best geometrical resolution available on these SANS instruments. At higher temperatures the width in the transverse direction begins to increase, while the radial width remains resolution limited. We have also taken a limited number of isothermal measurements, and have found that above a certain (H,T) the intensity and positions of the peaks are reversible, while below they are irreversible. The onset of transverse broadening is very close to where we observe this crossover from reversible to irreversible behavior in this sample, and thus we associate this broadening with the irreversibility line and melting identified in bulk measurements. We note that the scattering still has sixfold symmetry as clearly shown in the 6.5 K data of Fig. 2(a), while an isotropic vortex liquid would exhibit a ring of uniform intensity as a function of ϕ rather than the sixfold pattern observed. We have noted in our experiments that the observed vortex pattern is locked by the (weak) crystalline anisotropy, in that we find a vortex pattern with the same orientation as shown in Fig. 1 for a variety of directions of the field with respect to the crystal axes. Thus we describe this phase as a correlated flux fluid, where the orientation of the vortex pattern continues to be controlled by this anisotropy. The radial positions of the peaks are determined by the average vortex spacing, and we detect no increase in the radial width in this temperature regime. In the case of hexatic liquids typically both transverse and longitudinal widths are observed, and are coupled [15]. The transition is also expected to be first order, and thus these argue against the interpretation of a hexatic fluid for Nb. We see from Fig. 3 that an intrinsic radial width is only observed close to T_c, but even here the sixfold symmetry is still preserved. Indeed, we find no evidence of an isotropic liquid ring of scattering under any conditions.

The phase diagram we have determined is shown in Fig. 4. The H_{c2} phase boundary is determined by three separate sets of measurements. The open circles are superconducting quantum interference device (SQUID) measurements taken on a small piece cut from the end of the crystal [16], with H_{c2} defined as the onset of bulk diamagnetism [13]. The solid circles are obtained from our $I(T)$ data, while the solid squares are determined by the field where the isothermal scattering vanishes. Good agreement is obtained between these data, demonstrating that within our experimental sensitivity the vortex scattering disappears at H_{c2}. We also show the field where the flux begins to penetrate the sample, which is identified as the sudden onset of vortex scattering as H increases beyond $\frac{1}{2}H_{c1}$ (after zero-field cooling), where the $\frac{1}{2}$ comes from the demagnetization factor for our sample geometry. In the local limit we estimate $\kappa \approx (H_{c2}/H_{c1})^{1/2} \approx 2$. This is considerably above the value of $\kappa \approx 0.8$ obtained in very high purity and defect-free Nb [17], but considerably smaller than κ obtained on sputtered films [13] (≈ 10), or cold-rolled foils [12] (~ 7), where melting curves have been identified.

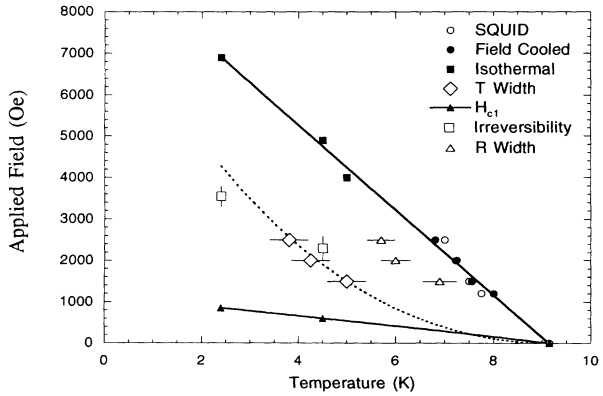

FIG. 4. Phase diagram determined for Nb (see text).

The irreversibility line (open squares) as determined by our isothermal measurements, the onset temperature of the intrinsic transverse widths (open diamonds), and the onset of the radial widths (open triangles), are also shown in Fig. 4. It is clear that the irreversibility line and transverse Q broadening occur in close proximity to each other, and well below H_{c2}, and we thus associate this with the irreversibility (melting) curve identified in bulk measurements. The dotted curve is a fit to a melting curve for comparison purposes [18]. We note that our irreversibility curve is substantially below that of Drulis *et al.* [12] obtained on the higher κ cold-rolled foils, and their curve is below that found by Schmidt, Israeloff, and Goldman for high κ sputtered films [13], supporting the expectation that T_{irr} depends on the defect density and/or pinning strength in the material.

The temperature dependence of the widths of the vortex peaks must originate from the vortex dynamics, and there are two alternative explanations for our data. The first is that the development of the transverse widths, coupled with the irreversibility line we observe, signals a transition to an orientationally disordered or hexatic vortex phase. At a higher temperature the development of intrinsic radial widths indicates that translational symmetry is lost. The implication is that there are three vortex regimes: a crystalline phase at low T, an orientationally disordered phase at intermediate T, and a correlated flux fluid in the high T regime.

A second possible interpretation is that the transverse width originates from strong inelastic scattering associated with the soft shear mode of the vortex lattice—the same mode that would be involved in melting [7–9]. Thus with sufficiently high resolution the elastic and inelastic scattering could be distinguished; one would have to assume that these are convolved into a single broadened peak given the present resolution. This interpretation implies that the lattice has not yet melted with the onset of transverse broadening, in which case the observed irreversibility curve would not be associated with melting. The melting would instead be identified with a transition to a fluid phase where the radial widths in-

crease. This would correspond more closely to the melting line identified in bulk measurements on high κ samples [12,13], and would suggest that the melting curve is not strongly dependent on κ.

We favor the first interpretation based on the abrupt onset of the transverse widths coupled with our own irreversibility data, but we cannot unambiguously rule out the second. However, in either scenario we have found that the basic sixfold symmetry is preserved throughout. If this vortex correlation originates from the underlying crystal symmetry then an isotropic liquid would only be observed if the crystalline anisotropy were negligible. In all other cases a correlated flux liquid is realized.

We thank C. J. Glinka and S. Krueger for their generous assistance with the data collection and analysis programs, R. W. Erwin and L. Santodonato for their assistance with the superconducting magnet system, J. L. Peng for his assistance with the SQUID measurements, and J. J. Rush for providing the crystal. We also thank R. J. Birgeneau, H. R. Glyde, and D. R. Nelson for helpful conversations. The research at Maryland is supported by the NSF, DMR 93-02380. The NG-3 SANS is supported by the NSF, DMR 91-22444.

[1] K. A. Müller, M. Takashige, and J. G. Bednorz, Phys. Rev. Lett. **58**, 1143 (1987).

[2] For a recent review, see D. J. Bishop, P. L. Gammel, D. A. Huse, and C. A. Murray, Science **255**, 165 (1992).

[3] E. M. Forgan, D. McK. Paul, H. A. Mook, P. A. Timmins, H. Keller, S. Sutton, and J. S. Abell, Nature (London) **343**, 735 (1990); M. Yethiraj, H. A. Mook, G. D. Wignall, R. Cubitt, E. M. Forgan, D. M. Paul, and T. Armstrong, Phys. Rev. Lett. **70**, 857 (1993).

[4] B. Keimer, I. Aksay, F. Dogan, R. W. Erwin, J. W. Lynn, and M. Sarikaya, Science **262**, 83 (1993).

[5] S. Safar, P. L Gammel, D. A. Huse, D. J. Bishop, W. C. Lee, J. Giapintzakis, and D. M. Ginsberg, Phys. Rev. Lett. **70**, 3800 (1993).

[6] A. Schilling, R. Jin, J. D. Guo, and H. R. Ott, Phys. Rev. Lett. **71**, 1899 (1993).

[7] D. S. Fisher, M. P. A. Fisher, and D. A. Huse, Phys. Rev. B **43**, 130 (1991).

[8] G. Blatter and B. Ivlev, Phys. Rev. Lett. **70**, 2621 (1993).

[9] J. A. O'Neill and M. A. Moore, Phys. Rev. Lett. **69**, 2582 (1992); H. R. Glyde, K. K. Moleko, and P. Findeisen, Phys. Rev. B **45**, 2409 (1992); J. Hu and A. H. MacDonald, Phys. Rev. Lett. **71**, 432 (1993); Y. Kato and N. Nagaosa, Phys. Rev. B **48**, 7383 (1993); G. Carneiro, R. Cavalcanti, and A. Gartner, Phys. Rev. B **47**, 5263 (1993).

[10] D. R. Nelson, in *Phenomenology and Applications of High Temperature Superconductors*, edited by K. S. Bedell *et al.* (Addison-Wesley, Reading, MA, 1992).

[11] M. Suenaga, A. K. Ghosh, Y. Xu, and D. O. Welch, Phys. Rev. Lett. **66**, 1777 (1991).

[12] H. Drulis, Z. G. Xu, J. W. Brill, L. E. De Long, and J.-C. Hou, Phys. Rev. B **44**, 4731 (1991).

[13] M. F. Schmidt, N. E. Israeloff, and A. M. Goldman, Phys. Rev. Lett. **70**, 2162 (1993); Phys. Rev. B **48**, 3404 (1993).

[14] For a description of neutron scattering from vortices and early work in Nb, see J. Schelten, H. Ullmaier, and W. Schmatz, Phys. Status Solidi (b) **48**, 619 (1971); D. K. Christen, H. R. Kerchner, S. T. Sekula, and P. Thorel, Phys. Rev. B **21**, 102 (1980).

[15] J. D. Brock, R. J. Birgeneau, J. D. Litster, and A. Aharony, Contemp. Phys. **30**, 321 (1989).

[16] Attempts were made to measure the irreversibility line, but we found that cutting the crystal introduced sufficient strains and defects to affect the results, while the full crystal is too large to be accommodated in the SQUID system. We therefore undertook our own isothermal measurements to determine the irreversibility line with neutrons.

[17] H. W. Weber, E. Seidl, C. Laa, E. Schachinger, M. Prohammer, A. Junod, and D. Eckert, Phys. Rev. B **44**, 7585 (1991).

[18] A. Houghton, R. A. Pelcovits, and A. Sudbø, Phys. Rev. B **40**, 6763 (1989).

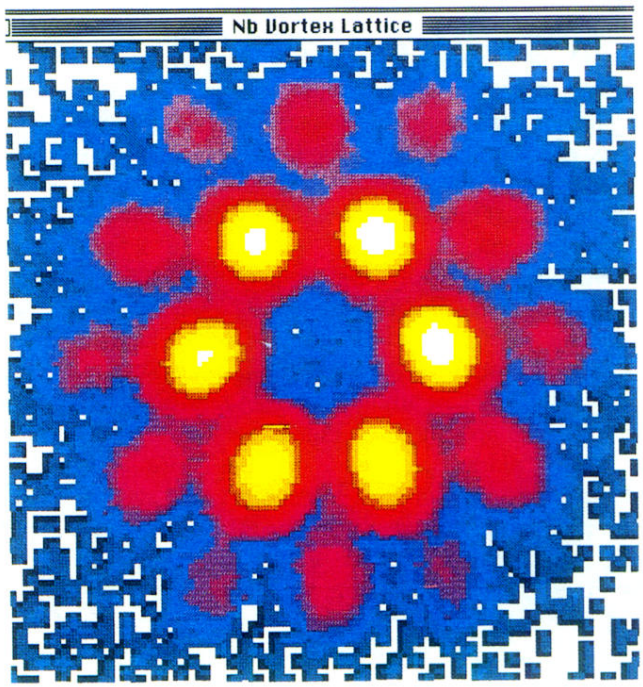

FIG. 1. Image on the two-dimensional SANS detector, taken with relatively coarse resolution. The log of the scattered neutron intensity has been mapped into a color spectrum. The six-fold pattern of first-order peaks has the strongest intensity, with higher order peaks having weaker intensities.